Integral transform solution of random coupled parabolic partial differential models

María Consuelo Casabán[1] | **Rafael Company**[1] | **Vera N. Egorova**[2] | **Lucas Jódar**[1]

[1]Instituto de Matemática Multidisciplinar, Universitat Politècnica de València, Valencia, Spain
[2]Departamento de Matemática Aplicada y Ciencias de la Computació, Universidad de Cantabria, Santander, Spain

Correspondence
María Consuelo Casabán, Instituto de Matemática Multidisciplinar, Universitat Politècnica de València, Camino de Vera, s/n, 46022 Valencia, Spain.
Email: macabar@imm.upv.es

Random coupled parabolic partial differential models are solved numerically using random cosine Fourier transform together with non-Gaussian random numerical integration that captures the highly oscillatory behaviour of the involved integrands. Sufficient condition of spectral type imposed on the random matrices of the system is given so that the approximated stochastic process solution and its statistical moments are numerically convergent. Numerical experiments illustrate the results.

KEYWORDS

random cosine Fourier transform, random coupled parabolic partial differential system, random oscillatory integration, random spectral analysis

MSC CLASSIFICATION

35R60; 60H15; 60H35; 62M15; 65D30; 65R10; 68U20

1 | INTRODUCTION

Random time-dependent scalar mean square partial differential models have been treated recently from both the theoretical and numerical points of view, because in real problems, the parameters, coefficients and initial/boundary conditions are subject to uncertainties, not only by error measurement but also to the difficulty of access to the measurement, the possible heterogeneity of the materials or media and so forth. Spatial uncertainty models described by random elliptic PDEs in bounded domains are treated in Bäck et al,[1] Bachmayr et al[2] and Ernst et al[3] using spectral Galerkin and collocation methods. In dealing with the coupled partial differential models, the uncertainties are involved in the matrix coefficients or vector initial/boundary conditions.

Coupled partial differential models are frequent in several engineering disciplines such as geomechanics,[4] geotechnics,[5] microwave heating processes,[6] optics,[7] ocean models[8,9] and so forth. They also appear in plasma fusion models,[10] cardiology[11,12] or species population dynamics.[13]

Solving random models presents somewhat unexpected peculiarities not presented in the deterministic case. In fact, in the random case, it is important not only the determination of the exact or approximate stochastic process solution but also the computation of its statistical moments, mainly the expectation and the standard deviation.

Using iterative methods involves the storage of high computational complexity of all the previous levels of iteration and usually the methods become unmanageable.[14] This motivates the search of alternative methods with as simple as possible expressions of the stochastic solution process. In a recent paper,[15] one uses Fourier transforms together with the random Gaussian quadrature rules to approximate stochastic process solution. The method proposed in Casabán

et al[15] has the advantage that approximate stochastic solution is simple and the computation of its statistical moments are manageable; however, as the numerical integration is based on Gaussian quadrature rules, the accuracy decreases for highly oscillatory Fourier kernels in large domains.[16-18] In this paper, the above-mentioned drawback is overcome by taking an appropriate truncation of the infinite integral and using quadrature rules with good behaviour dealing with highly oscillatory integrands.

PDE models in unbounded domains using Fourier integral transforms have been treated in Jódar and Goberna.[19,20] This paper deals with a more general random coupled parabolic problem

$$\frac{\partial u(z,t)}{\partial t}(\xi) = A(\xi)u(z,t)(\xi) + B(\xi)\frac{\partial^2 u(z,t)}{\partial z^2}(\xi),\ z>0,\ t>0\ , \tag{1}$$

$$u(z,0)(\xi) = f(z)(\xi),\ z>0,\ \xi\in\Omega, \tag{2}$$

$$\frac{\partial u}{\partial z}(0,t)(\xi) = g(t)(\xi),\ t>0,\ \xi\in\Omega, \tag{3}$$

$$\lim_{z\to\infty} u(z,t)(\xi) = 0,\ \lim_{z\to\infty}\frac{\partial u}{\partial z}(z,t)(\xi) = 0, \tag{4}$$

where $u(z,t)(\xi) = [u_1(z,t)(\xi), u_2(z,t)(\xi)]^T \in \mathbb{R}^2$, $g(t)(\xi) = [g_1(t)(\xi), g_2(t)(\xi)]^T$, $f(z)(\xi) = [f_1(z)(\xi), f_2(z)(\xi)]^T$, and

$$A(\xi) = \left(a_{ij}(\xi)\right)_{1\le i,j\le 2},\ B(\xi) = \left(b_{ij}(\xi)\right)_{1\le i,j\le 2}. \tag{5}$$

Here, $A(\xi)$ and $B(\xi)$ are random matrices, $f(z)(\xi)$ and $g(t)(\xi)$ are stochastic processes (s.p.'s) with properties to be specified later. We assume that for each event $\xi\in\Omega$, the sample matrix $B(\xi)$ satisfies

$$\lambda_{\min}\left(\frac{B(\xi)+B(\xi)^T}{2}\right) = b(\xi) > 0, \tag{6}$$

where $\lambda_{\min}$ denotes the minimum eigenvalue.

This paper is organized as follows. Section 2 deals with the solution of the simplified deterministic problem after taking sample realizations for each event $\xi\in\Omega$. Matrix analysis of involved matrices $A(\xi)$ and $B(\xi)$ is performed in order to determine the spectral sufficient condition to guarantee the convergence.

The unsuitable use of Gaussian quadrature for cosine oscillatory integrals and the convergence of the truncated integrals suggest the introduction of alternative quadrature formulae such as the midpoint Riemann sum (see Davis and Rabinowitz,[21] Section 3.9 or the trapezoidal rule).

In Section 3, the random case is addressed taking into account the ideas of previous section in order to construct random approximate solution s.p.'s that make manageable the computation of its statistical moments, in particular, the expectation and the variance. Simulations show the efficiency of the proposed numerical methods.

2 | SOLVING THE SAMPLED DETERMINISTIC CASE

For the sake of clarity in the presentation, let us recall some algebraic concepts, notations and results.

If P is a matrix in $\mathbb{R}^{N\times N}$, its logarithmic operator norm $\mu(P)$ is defined by

$$\mu(P) = \max\left\{\lambda;\ \lambda \text{ eigenvalue of } \frac{P+P^T}{2}\right\}. \tag{7}$$

By Dahlquist,[22] the matrix exponential e^{Pt} satisfies $||e^{Pt}|| \le e^{t\mu(P)}, t\ge 0$.

Lemma 1. *Let $B\in\mathbb{R}^{N\times N}$ be a matrix such that $B+B^T$ is positive definite and satisfies (6). Then,*

$$\mu(A-\omega^2 B) \le \mu(A) - b\omega^2,\ b = \lambda_{\min}\left(\frac{B+B^T}{2}\right),\ \omega>0\ . \tag{8}$$

Proof. Let $\omega>0$, and let us write

$$\frac{(A-B\omega^2)+(A-B\omega^2)^T}{2} = \frac{A+A^T}{2} - \omega^2\left(\frac{B+B^T}{2}\right). \tag{9}$$

As $\frac{A+A^T}{2}$ and $-\omega^2\left(\frac{B+B^T}{2}\right)$ are both symmetric matrices, by Ostrowski theorem (see Ostrowski[23]), each eigenvalue λ of matrix (9) satisfies

$$\lambda \leq \lambda_{\max}\left(\frac{A+A^T}{2}\right) - \omega^2\lambda_{\min}\left(\frac{B+B^T}{2}\right) = \mu(A) - b\omega^2, \tag{10}$$

where b is given by (6). Hence, the result is established. □

If $f(z) = [f_1(z), f_2(z)]^T$ is absolutely integrable in $[0,\infty)$, then the cosine Fourier transform of $f(z)$ is defined by

$$\mathcal{F}_c[f](\omega) = \int_0^\infty f(z)\cos(\omega z)dz,\ \omega \geq 0, \tag{11}$$

and if $f(z)$ is twice differentiable and $f''(z) = [f_1''(z), f_2''(z)]^T$ is absolutely integrable, then

$$\mathcal{F}_c[f''](\omega) = -\omega^2\mathcal{F}_c[f](\omega) - f'(0),\ \omega \geq 0. \tag{12}$$

In order to simplify the notation, in the following content of this section, we will denote for a realization of random matrices $A(\xi)$ and $B(\xi)$ as A and B, respectively. For the sake of coherence, we also denote $f(z)$, $g(t)$ and $u(z,t)$ as the corresponding realizations for a fixed event $\xi \in \Omega$.

In order to obtain a candidate solution of problems (1)–(6), let us apply the cosine Fourier transform $\mathcal{F}_c$ regarding $u = u(\cdot,t)$ as an absolute integrable function of the active variable $z > 0$. Let us denote

$$V(t) = \mathcal{F}_c[u(\cdot,t)](\omega) = \int_0^\infty u(z,t)\cos(\omega z)dz,\ \omega > 0, \tag{13}$$

and applying $\mathcal{F}_c$ to (1) and taking into account (12), one gets

$$\mathcal{F}_c\left[\frac{\partial^2 u}{\partial z^2}(\cdot,t)\right](\omega) = -\omega^2\mathcal{F}_c[u(\cdot,t)](\omega) - \frac{\partial u}{\partial z}(0,t) = -\omega^2 V(t)(\omega) - g(t), \tag{14}$$

$$V(0) = \mathcal{F}_c[u(0,t)](\omega) = \mathcal{F}_c[f(z)](\omega) = F(\omega). \tag{15}$$

Hence, $V(t)(\omega)$ is the solution of the initial value problem in time,

$$\frac{d}{dt}V(t)(\omega) = (A - \omega^2 B)V(t)(\omega) - Bg(t),\ t > 0,\ \omega > 0 \text{ fixed},\ V(0)(\omega) = F(\omega). \tag{16}$$

The solution of (16) for $\omega > 0$ fixed takes the form

$$V(t)(\omega) = e^{(A-\omega^2 B)t}\left\{F(\omega) - \int_0^t e^{-(A-\omega^2 B)s}c(s)ds\right\},\ c(s) = Bg(s). \tag{17}$$

Under hypothesis of Lemma 1, and continuity of $g(t)$, taking cosine inverse $\mathcal{F}_c^{-1}$, one gets

$$u(z,t) = \mathcal{F}_c^{-1}[V(t)(\omega)] = \frac{2}{\pi}\int_0^\infty e^{(A-\omega^2 B)t}F(\omega)\cos(\omega z)d\omega = \frac{2}{\pi}(I_1 - I_2), \tag{18}$$

where

$$I_1 = \int_0^\infty e^{(A-\omega^2 B)t}F(\omega)\cos(\omega z)d\omega,\ I_2 = \int_0^\infty\left(\int_0^t e^{(A-\omega^2 B)(t-s)}c(s)\cos(\omega z)ds\right)d\omega. \tag{19}$$

Integrals (19) can be truncated for ω, getting the approximations

$$I_1(R) = \int_0^R e^{(A-\omega^2 B)t}F(\omega)\cos(\omega z)d\omega,\ I_2(R) = \int_0^R\left(\int_0^t e^{(A-\omega^2 B)(t-s)}c(s)\cos(\omega z)ds\right)d\omega,\ R > 0 \tag{20}$$

and the approximate solution $u_R(z,t) = \frac{2}{\pi}\left(I_1(R) - I_2(R)\right),\ z > 0,\ t > 0$.

Now we prove that $\{u_R(z,t)\}$ is convergent and that $\lim_{R\to\infty}u_R(z,t) = u(z,t)$, stating that

$$u(z,t) - u_R(z,t) = \frac{2}{\pi}\left(J_1(R) - J_2(R)\right)\xrightarrow[R\to\infty]{0}, \tag{21}$$

where

$$J_1(R)=\int_R^\infty e^{(A-\omega^2B)t}F(\omega)\cos(\omega z)d\omega,\ J_2(R)=\int_0^t\left(\int_R^\infty e^{(A-\omega^2B)(t-s)}c(s)\cos(\omega z)d\omega\right)ds. \tag{22}$$

Using Lemma 1, (22) and the substitution $u=\omega\sqrt{bt}$, one gets

$$\begin{aligned}||J_1(R)||&\le\int_R^\infty e^{\mu(A-\omega^2B)t}||F(\omega)||d\omega\le||F||_\infty\int_R^\infty e^{(\mu(A)-\omega^2b)t}d\omega=||F||_\infty e^{\mu(A)t}\int_R^\infty e^{-bt\omega^2}d\omega\\&=\frac{||F||_\infty e^{\mu(A)t}}{\sqrt{bt}}\int_{R\sqrt{bt}}^\infty e^{-u^2}du=\frac{||F||_\infty\sqrt{\pi}}{2\sqrt{bt}}e^{\mu(A)t}\mathrm{erfc}(R\sqrt{bt}),\end{aligned} \tag{23}$$

where $\sup\{||F(\omega)||;\ \omega\ge0\}=||F||_\infty$.

Also, from Lemma 1, for the second integral of (22), one gets

$$\|J_2(R)\|\le\int_0^t\left(\int_R^\infty e^{(\mu(A)-\omega^2b)(t-s)}\,\|B\|\,\|g(s)\|\,d\omega\right)ds=\|B\|\int_0^t\|g(s)\|\,e^{\mu(A)(t-s)}\left(\int_R^\infty e^{-\omega^2b(t-s)}d\omega\right)ds. \tag{24}$$

As we did in previous bound of $J_1(R)$ in (23), we have

$$\int_R^\infty e^{-\omega^2b(t-s)}d\omega=\frac{\sqrt{\pi}}{2\sqrt{b(t-s)}}\mathrm{erfc}\left(R\sqrt{b(t-s)}\right). \tag{25}$$

From (24) and (25), one concludes

$$\|J_2(R)\|\le\frac{\sqrt{\pi}\,\|B\|}{2\sqrt{b}}\int_0^t\frac{\|g(s)\|\,e^{\mu(A)(t-s)}}{\sqrt{t-s}}\mathrm{erfc}\left(R\sqrt{b(t-s)}\right)ds=\frac{\sqrt{\pi}\,\|B\|}{b}\int_0^{\sqrt{bt}}\left\|g\left(t-\frac{v^2}{b}\right)\right\|e^{\mu(A)\frac{v^2}{b}}\mathrm{erfc}\,(Rv)\,dv. \tag{26}$$

As $\lim_{x\to\infty}\mathrm{erfc}(x)=0$, and $g(t)$ is continuous and bounded in a bounded interval, from (23) and (26), it follows that

$$\lim_{R\to\infty}J_i(R)=0,\ i=1,2. \tag{27}$$

Hence, from (21) and (27), one gets $\lim_{R\to\infty}(u(z,t)-u_R(z,t))=0$.

Note also that $u(z,t)$ given by (18)–(19) is well defined because integrals I_1 and I_2 of (19) are absolutely integrable, because for $z>0$ and $t>0$ fixed, we have (see Lemma 1)

$$\|I_1\|\le\int_0^\infty e^{\mu(A)t}\,\|F(s)\|\,e^{-\omega^2bt}d\omega\le\|F\|_\infty e^{\mu(A)t}\int_0^\infty e^{-\omega^2bt}d\omega<+\infty,$$

$$\begin{aligned}\|I_2\|&\le\int_0^t\int_0^\infty e^{\mu(A)(t-s)-\omega^2b(t-s)}\,\|c(s)\|\,d\omega ds\le\|B\|\int_0^t\|g(s)\|\,e^{\mu(A)(t-s)}\left(\int_0^\infty e^{-\omega^2b(t-s)}d\omega\right)ds\\&=\frac{\|B\|}{\sqrt{b}}\int_0^t\frac{\|g(s)\|\,e^{\mu(A)(t-s)}}{\sqrt{t-s}}\left(\int_0^\infty e^{-v^2}dv\right)ds=\frac{\sqrt{\pi}\,\|B\|}{2\sqrt{b}}\int_0^t\frac{\|g(s)\|\,e^{\mu(A)(t-s)}}{\sqrt{t-s}}ds.\end{aligned}$$

In summary, the following result has been established.

Theorem 1. *Consider problems (1)–(4) for a fixed event $\xi\in\Omega$, where $f(z)$ is absolutely integrable, $g(t)$ is continuous and B satisfies condition (6) with $b>0$. Then*

1. *$u(z,t)$ given by (18)–(19) is solution of problems (1)–(4);*
2. *$u_R(z,t)=\frac{2}{\pi}(I_1(R)-I_2(R))$, $z>0$, $t>0$, where $I_1(R)$ and $I_2(R)$ are defined by (20), converges as $R\to\infty$ to $u(z,t)$ uniformly for $z>0$ and pointwise at each $(z,t)\in\mathbb{R}^+\times\mathbb{R}^+$.*

Example 2.1. Consider problems (1)–(4) for a realization corresponding to $\xi_0\in\Omega$ fixed with the data

$$A=\begin{bmatrix}0&a\\-a&0\end{bmatrix},\ B=\nu I=\begin{bmatrix}\nu&0\\0&\nu\end{bmatrix},\ a>0,\ \nu>0;\ u(z,0)=f(z)=\begin{bmatrix}0\\0\end{bmatrix},\ \frac{\partial u}{\partial z}(0,t)=\begin{bmatrix}-g(t)\\0\end{bmatrix}, \tag{28}$$

modelling the influence of the Earth's rotation on ocean currents,[8] whose exact solution takes the form

$$u_1(z,t)=\sqrt{\frac{\nu}{\pi}}\int_0^t \frac{g(s)}{\sqrt{t-s}}e^{-\left(\frac{z^2}{4\nu(t-s)}\right)}\cos\left(a(t-s)\right)ds,\ u_2(z,t)=-\sqrt{\frac{\nu}{\pi}}\int_0^t \frac{g(s)}{\sqrt{t-s}}e^{-\left(\frac{z^2}{4\nu(t-s)}\right)}\sin\left(a(t-s)\right)ds. \tag{29}$$

Here, variables t and z represent the time and depth coordinates, u_1 and u_2 describe the zonal and meridional surface ocean current velocities, a is the coriolis parameter and ν is the eddy parameterized vertical viscosity coefficient.

Note that in this case,

$$A-\omega^2 B=\begin{bmatrix}-\omega^2\nu & a\\ -a & -\omega^2\nu\end{bmatrix},\ \mu(A-\omega^2B)=\max\left\{\lambda\in\sigma\begin{bmatrix}-\omega^2\nu & 0\\ 0 & -\omega^2\nu\end{bmatrix}\right\}=-\omega^2\nu. \tag{30}$$

From (17) and (30), it follows that

$$c(s)=\nu\begin{bmatrix}-g(t)\\ 0\end{bmatrix};\ e^{(A-\omega^2B)t}=e^{-\omega^2\nu t}\begin{bmatrix}\cos(at) & \sin(at)\\ -\sin(at) & \cos(at)\end{bmatrix}. \tag{31}$$

By (18)–(19) and (31), the solution of the problem takes the form

$$u(z,t)=-\frac{2}{\pi}\int_0^\infty\int_0^t e^{(A-\omega^2B)(t-s)}c(s)\cos(\omega z)dsd\omega=\frac{2}{\pi}\int_0^\infty I_2(t,\omega)\cos(\omega z)d\omega, \tag{32}$$

where

$$I_2(t,\omega)=\int_0^t e^{-\omega^2\nu(t-s)}\nu g(s)\begin{bmatrix}\cos\left(a(t-s)\right)\\ -\sin\left(a(t-s)\right)\end{bmatrix}ds. \tag{33}$$

Taking advantage of the knowledge of the exact solution given by (29), we check that Gauss–Laguerre quadrature[15] of (32) provides wrong results for large values of z.

Let us take the data $a=1$, $\nu=1$ and $g(t)=1$. Note that in the case $g(t)=1$, expression (33) becomes

$$I_2(t,\omega)=\frac{\nu}{a^2+\nu^2\omega^4}\begin{bmatrix}\omega^2\nu+e^{-\omega^2\nu t}\left(a\sin(at)-\omega^2\nu\cos(at)\right)\\ -a+e^{-\omega^2\nu t}\left(a\cos(at)+\omega^2\nu\sin(at)\right)\end{bmatrix}. \tag{34}$$

Next, Table 1 shows the absolute errors when one approximates (29) using Gauss–Laguerre quadrature of several degrees M for $z=5$ and $t=1$.

The convergence of truncated integrals in Theorem 1 suggests the approximation of the truncated integrals using appropriate quadrature rules preserving the oscillatory behaviour. Let us denote

$$u_R(z,t)=\frac{2}{\pi}\int_0^R I_2(t,\omega)\cos(\omega z)d\omega. \tag{35}$$

M	AbsErr($u_1(5,1)$)	AbsErr($u_2(5,1)$)
1	2.7254$e-01$	1.2057$e-01$
2	7.4014$e-01$	3.5587$e-01$
3	2.2645$e-02$	1.0762$e-01$
4	4.4318$e-01$	9.7300$e-02$
5	4.5831$e-01$	1.5709$e-01$
6	3.6717$e-01$	2.1590$e-01$
7	5.1360$e-01$	1.8173$e-01$
8	1.9483$e-03$	5.3340$e-02$
9	1.3911$e-01$	6.4812$e-02$
10	4.8348$e-01$	1.3559$e-01$
11	3.3161$e-01$	1.2510$e-01$
12	2.1783$e-01$	6.6086$e-02$
13	1.4817$e-01$	8.2631$e-03$
14	2.3801$e-01$	5.7655$e-02$
15	2.8347$e-01$	7.0344$e-02$

TABLE 1 Absolute error of numerical approximation of (29) by using Gauss–Laguerre quadratures of degree M at $z=5$ and $t=1$

TABLE 2 Absolute errors of numerical approximations of (35) at $z = 5$, $t = 1$, by the midpoint Riemann sum with fixed $h = 0.05$

R	AbsErr($u_1(5,1)$)	AbsErr($u_2(5,1)$)
5	$2.2187e-04$	$6.0459e-06$
10	$6.6113e-05$	$1.1396e-06$
15	$9.6916e-05$	$4.9150e-07$
20	$9.3665e-05$	$2.4768e-07$
25	$8.4522e-05$	$1.3928e-07$
30	$7.4942e-05$	$8.4709e-08$

TABLE 3 Absolute errors of numerical approximations of (35) at $z = 5$, $t = 1$, by the midpoint Riemann sum with fixed $R = 20$ and various step size h

h	AbsErr($u_1(5,1)$)	AbsErr($u_2(5,1)$)
0.2000	$1.4793e-04$	$3.4924e-07$
0.1000	$1.4441e-05$	$5.0984e-08$
0.0500	$9.3665e-05$	$2.4768e-07$
0.0250	$1.3112e-04$	$3.4100e-07$
0.0125	$1.4912e-04$	$3.8592e-07$

TABLE 4 Root mean square errors (RMSEs) of numerical approximations of (35) by the midpoint Riemann sum with fixed $h = 0.05$ in the domain $(z,t) \in [0,5] \times [0,1]$ for the step sizes $\Delta z = 0.05$ and $\Delta t = 0.01$

R	RMSE ($u_1(z,t)$)	RMSE ($u_2(z,t)$)	CPU, s
5	$1.9717e-02$	$4.3759e-04$	0.6406
10	$8.0645e-03$	$4.2821e-05$	0.7188
15	$4.9310e-03$	$1.0860e-05$	2.1094
20	$3.5510e-03$	$4.1179e-06$	2.6406
25	$2.7871e-03$	$1.9559e-06$	2.0938
30	$2.3023e-03$	$1.0771e-06$	2.7969

The midpoint Riemann sum proposed in Davis and Rabinowitz,[21] Section 3.9 applied to (35) gives the approximation

$$u_R(z,t) \approx \frac{2h}{\pi} \sum_{j=0}^{N-1} I_2\left(t, \left(j+\frac{1}{2}\right)h\right) \cos\left(\left(j+\frac{1}{2}\right)hz\right), \tag{36}$$

where $Nh = R$.

The numerical convergent of the proposed midpoint Riemann sum approximation of the solution given by (36) is studied with respect to the involved parameters R, N and h in Tables 2 and 3. In particular, in Table 2, we fix the value of h and vary R in order to analyse the impact of the truncation point R. As expected, increasing values of R result in smaller absolute error. In Table 3, R is fixed and the step-size discretization h is changing.

In order to compare the numerical approximation by the Riemann midpoint sum with the analytical solution (29) in an entire computational domain, we calculate the root mean square error (RMSE). The results for fixed $h = 0.05$ at the fixed computational domain $0 \le t \le 1$, $0 \le z \le 5$ are presented in Table 4 and plotted in Figure 1. Because the step size is fixed, the total computational time varies depending on the size of the integration domain, that is, on the values

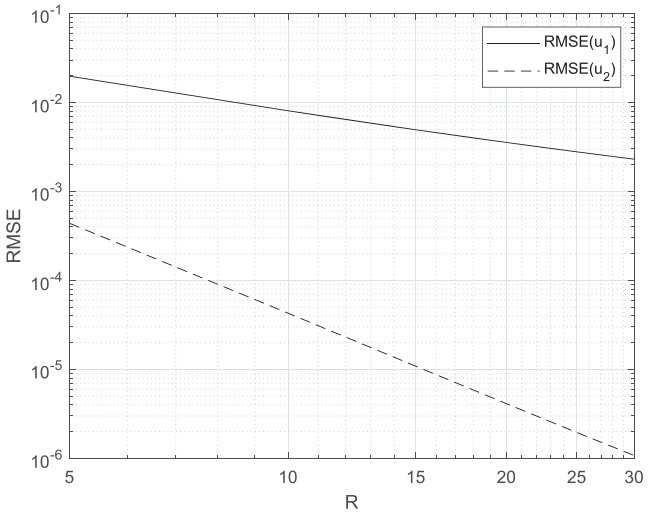

FIGURE 1 RMSE of numerical approximations of (35) by the midpoint Riemann sum with fixed $h = 0.05$ for various values of R in the domain $(z,t) \in [0,5] \times [0,1]$ for the step sizes $\Delta z = 0.05$ and $\Delta t = 0.01$. RMSE, root mean square error

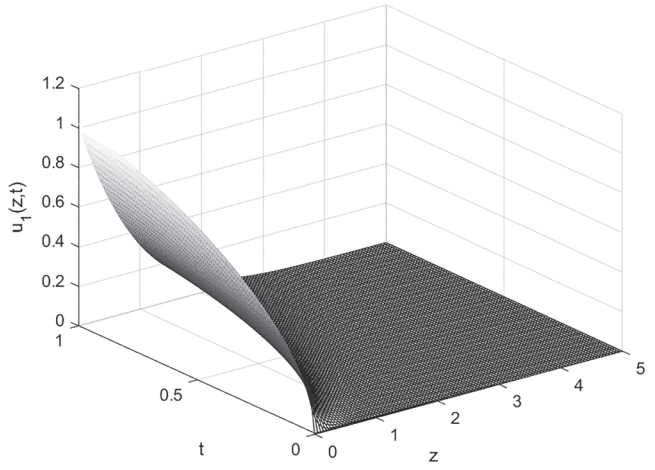

FIGURE 2 Solution $u_1(z,t)$ calculated by (29) for $a = \nu = 1, g(t) = 1$

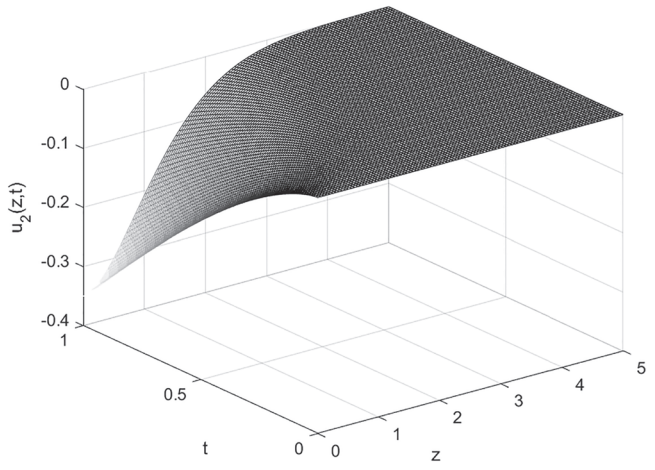

FIGURE 3 Solution $u_2(z,t)$ calculated by (29) for $a = \nu = 1, g(t) = 1$

of R. The CPU time of each simulation is reported in Table 4 as well. The solutions $u_1(z,t)$ and $u_2(z,t)$ of Example 2.1 are presented in Figures 2 and 3, respectively. Computations have been carried out by MATLAB© R[24] for Windows 10 home (64-bit) Intel(R) Core(TM) i5-8265u CPU, 1.60 GHz.

3 | THE RANDOM CASE: NUMERICAL SOLUTION AND NUMERICAL CONVERGENCE

In Section 2, for a fixed realization corresponding to some $\xi_0 \in \Omega$, we have confirmed that Gaussian quadrature is not appropriate for approximating oscillatory integrals of the cosine inverse Fourier transform (see Example 2.1). Then, we experimented in Section 2 the alternative of truncation combined with midpoint Riemann sum in the truncated domain $[0, R]$. In this section, we only choose this technique to approximate the solution s.p. of problems (1)–(4), as well as the computation of the expectation and variance of the approximate s.p.

For the sake of clarity in the presentation, we recall some notation about s.p. used in previous paper[15] and references therein.

Let $(\Omega, \mathfrak{F}, \mathbb{R})$ be a complete probability space, and let $L_p^{m\times n}(\Omega)$ be a set of all random matrices $Y = (y_{ij})_{m\times n}$, whose entries y_{ij} are r.v.'s satisfying

$$\left\|y_{ij}\right\|_p = \left(\mathbb{E}[|y_{ij}|^p]\right)^{1/p} < +\infty,\ p \geq 1, \tag{37}$$

which means that $y_{ij} \in L_p(\Omega)$, where $\mathbb{E}[\cdot]$ denotes the expectation operator. The space of all random matrices of size $m\times n$, endowed with the matrix $p-$norm, $\left(L_p^{m\times n}(\Omega), \|\cdot\|_p\right)$, defined by

$$\|Y\|_p = \sum_{i=1}^{m}\sum_{j=1}^{n}\left\|y_{ij}\right\|_p,\ \mathbb{E}[|y_{ij}|^p] < +\infty, \tag{38}$$

is a Banach space. The definition of the matrix $p-$norm in (38) can be extended to matrix s.p.'s $Y(t) = \left(y_{ij}(t)\right)_{m\times n}$ of $L_p^{m\times n}(\Omega)$, where now each entry $\left(y_{ij}(t)\right)$ is an s.p., that is, $y_{ij}(t)$ is an r.v. for each t. We say that the matrix s.p. $Y(t)$ lies in $L_p^{m\times n}(\Omega)$, if $\left(y_{ij}(t)\right) \in L_p(\Omega)$ for every $1 \leq i \leq m, 1 \leq j \leq n$.

The definitions of integrability, continuity and differentiability of a matrix function lying in $L_p^{m\times n}(\Omega)$ follows in a natural manner using matrix $p-$norm introduced in (38). The case mean square corresponds to $p = 2$ and mean four $p = 4$. One has $L_4^{m\times n}(\Omega) \subset L_2^{m\times n}(\Omega)$ (see Casabán et al[15]).

Consider that a constant random matrix $L \in L_{2p}^{n\times n}(\Omega)$, $Y_0 \in L_{2p}^{n\times 1}(\Omega)$ and $C(s)$ lie in $L_{2p}^{n\times 1}(\Omega)$ and $2p-$ integrable. Assume that random matrix $L = \left(\ell_{ij}\right)_{n\times n}$ satisfies the moment condition

$$\mathbb{E}[|\ell_{ij}|^r] \leq m_{ij}(h_{ij})^r < +\infty, \ \forall r \geq 0, \ \forall i, j \ : \ 1 \leq i, j \leq n. \tag{39}$$

Then, by Casabán et al,[15] Section 3 the corresponding solution of the mean square initial value problem

$$Y'(s) = LY(s) + C(s), \ Y(0) = Y_0, \ s \geq 0 \tag{40}$$

is given by

$$Y(s) = e^{Ls}\left(Y_0 + \int_0^s e^{-Lv}C(v)\, dv\right). \tag{41}$$

Now for the sake of clarity, in the presentation, we list the conditions of the random parabolic partial differential systems (1)–(4). First, random matrices

$$A(\xi) \in L_4^{2\times 2}(\Omega), \ B(\xi) \in L_8^{2\times 2}(\Omega) \tag{42}$$

and satisfy the moment condition (39). In addition, assume that $g(t)(\xi) \in L_8^{2\times 1}(\Omega)$ for each $t > 0$ and it is continuous in $L_8^{2\times 1}(\Omega)$. Furthermore, assume that s.p. $f(z)(\xi) \in L_8^{2\times 1}(\Omega)$ for each $z > 0$ and it is absolutely integrable in $L_8^{2\times 1}(\Omega)$, then the random cosine Fourier transform of $f(z)(\xi)$, $F(\omega)(\xi)$, lies in $L_8^{2\times 1}(\Omega)$. Assume the random spectral condition: there exists $b^* > 0$ such that

$$\inf_{\xi\in\Omega} \lambda_{\min}\left(\frac{B(\xi) + B(\xi)^T}{2}\right) \geq b^* > 0. \tag{43}$$

Then, the random initial value problem (see 16)

$$\frac{d}{dt}V(t,\xi)(\omega) = (A(\xi) - \omega^2 B(\xi))V(t,\xi)(\omega) - B(\xi)g(t)(\xi), \ V(0,\xi)(\omega) = F(\omega) \tag{44}$$

has the mean square solution

$$V(t,\xi)(\omega) = e^{(A(\xi)-\omega^2B(\xi))\ t}\left(F(\omega)(\xi) - \int_0^t e^{-(A(\xi)-\omega^2B(\xi))\ s}c(s)(\xi)ds\right), \ c(s)(\xi) = B(\xi)g(s)(\xi), \tag{45}$$

and $V(t,\xi)$ lies in $L_2^{2\times 1}(\Omega)$. Using random cosine inverse transform (see 18), one has

$$u(z,t)(\xi) = \frac{2}{\pi}\int_0^\infty V(t,\xi)(\omega)\cos(\omega z)d\omega, \ \xi \in \Omega. \tag{46}$$

Truncation gives the approximate s.p.

$$u_R(z,t)(\xi) = \frac{2}{\pi}\int_0^R V(t,\xi)(\omega)\cos(\omega z)d\omega, \ \xi \in \Omega. \tag{47}$$

Using $N-$ midpoint Riemann sum quadrature of $u_R(z,t)(\xi)$, one gets

$$\mathrm{Mid}_N\left(u_R(z,t)(\xi)\right) = \frac{2h}{\pi}\sum_{j=0}^{N-1} V(t,\xi)\left(\omega_{j+\frac{1}{2}}\right)\ \cos\left(\omega_{j+\frac{1}{2}}z\right), \tag{48}$$

where $Nh = R$, $\omega_{j+\frac{1}{2}} = \left(j + \frac{1}{2}\right)h$.

Because the randomness of the integrand of (47) only affects to $V(t,\xi)(\omega)$, it is easy to check that

$$\mathbb{E}\left[\mathrm{Mid}_N\left(u_R(z,t)(\xi)\right)\right] = \frac{2h}{\pi}\sum_{j=0}^{N-1}\cos\left(\omega_{j+\frac{1}{2}}z\right)\mathbb{E}\left[V(t,\xi)\left(\omega_{j+\frac{1}{2}}\right)\right], \tag{49}$$

where

$$\begin{aligned}\mathrm{Var}\left[\mathrm{Mid}_N\ \left(u_R(z,t)(\xi)\right)\right] &= \mathbb{E}\left[\left(\mathrm{Mid}_N\ \left(u_R(z,t)(\xi)\right)\right)^2\right] - \mathbb{E}[\mathrm{Mid}_N\ \left(u_R(z,t)(\xi)\right)]^2 \\ &= \frac{4h^2}{\pi^2}\sum_{i=0}^{N-1}\sum_{j=0}^{N-1}\cos\left(\omega_{i+\frac{1}{2}}z\right)\cos\left(\omega_{j+\frac{1}{2}}z\right)\mathrm{Cov}\left[V(t,\xi)\left(\omega_{i+\frac{1}{2}}\right),\ V(t,\xi)\left(\omega_{j+\frac{1}{2}}\right)\right], \end{aligned} \tag{50}$$

where $\mathrm{Cov}[P,Q] = \mathbb{E}[PQ] - \mathbb{E}[P]\mathbb{E}[Q]$.

In an analogous way, the random trapezoidal quadrature rule can be used to approximate the random integral (47) obtaining the following expressions for the expectation and the variance of the approximate solution s.p. of (1)–(6)

$$\mathbb{E}\left[\mathrm{Trap}_N(u_R(z,t)(\xi))\right] = \frac{2\,h}{\pi}\left[\frac{1}{2}\,\mathbb{E}\left[V(t,\xi)(w_0)\right] + \sum_{k=1}^{N}\mathbb{E}\left[V(t,\xi)(w_k)\ \cos(w_k\ z)\right]\right], \tag{51}$$

$$\begin{aligned}\mathrm{Var}\left[\mathrm{Trap}_N(u_R(z,t)(\xi))\right] &= \mathbb{E}\left[\left(\mathrm{Trap}_N\left(u_R(z,t)(\xi)\right)\right)^2\right] - \mathbb{E}\left[\mathrm{Trap}_N\left(u_R(z,t)(\xi)\right)\right]^2 \\ &= \frac{4h^2}{\pi^2}\sum_{k=0}^{N}\sum_{\ell=0}^{N}\gamma_k\gamma_\ell\cos(w_k z)\cos(w_\ell z)\mathrm{Cov}\left[V(t,\xi)(w_k), V(t,\xi)(w_\ell)\right],\ \gamma_0 = \frac{1}{2},\ \gamma_k = 1,\ 1\le k\le N, \end{aligned} \tag{52}$$

where $Nh = R$, $w_\ell = \ell\,h$, $0\ \le\ \ell\ \le\ N$.

Algorithm 1 summarizes the steps to compute the approximations of the expectation and the standard deviation of the solution s.p. (46)

Algorithm 1 Procedure to compute the expectation and the standard deviation of the approximate solution s.p. $\mathrm{Mid}_N\left(u_R(z,t)(\xi)\right)$ (48) of the problems (1)–(4).

Take random matrices $A(\xi) \in L_4^{2\times 2}(\Omega)$ and $B(\xi) \in L_8^{2\times 2}(\Omega)$ and check that all their entries satisfy the moment condition (39).
Take a continuous s.p. $g(t)(\xi)$ in $L_8^{2\times 1}(\Omega)$ for $t > 0$.
Take an absolutely integrable s.p. $f(z)(\xi)$ in $L_8^{2\times 1}(\Omega)$ for $z > 0$.
Check that the random spectral condition (43) is verified.
Fix a point (z,t), with $z > 0$, $t > 0$.
Choose the length of the truncation endpoint R and the number of subintervals N.
Compute the step size h using the relationship $Nh = R$.
for $j = 0$ to $j = N-1$ **do**
  compute the $N-$ midpoints $\omega_{j+\frac{1}{2}}$ and the functions $\cos\left(\omega_{j+\frac{1}{2}}z\right)$.
end for
Choose and carry out a number K of realizations, $\xi = \{1,\dots,K\}$, over the r.v.'s involve in the random matrices $A(\xi)$ and $B(\xi)$ and the s.p.'s $g(t)(\xi)$ and $f(z)(\xi)$.
for each realization $\xi = 1$ to $\xi = K$ **do**
  Compute the Fourier cosine transform of $f(z)(\xi)$: $F(\omega)(\xi)$.
end for
for $j = 0$ to $j = N-1$ **do**
  for $\xi = 1$ to $\xi = K$ **do**
    Compute the deterministic expression (45) with $\omega = \omega_{j+\frac{1}{2}}$.
  end for
  Compute the mean of the K values obtained.
end for
Compute the approximation of the expectation, $\mathbb{E}[\mathrm{Mid}_N\left(u_R(z,t)(\xi)\right)]$ using expression (49) or $\mathbb{E}[\mathrm{Trap}_N\left(u_R(z,t)(\xi)\right)]$ using (51).
Compute the approximation of the standard deviation, $\sqrt{\mathrm{Var}[\mathrm{Mid}_N\left(u_R(z,t)(\xi)\right)]}$ using expression (50) or $\sqrt{\mathrm{Var}[\mathrm{Trap}_N\left(u_R(z,t)(\xi)\right)]}$ using (52).

In the next example, we consider a random version of Example 2.1 where the uncertainty in the computation of the exact values of coriolis and eddy viscosity is considered. Another uncertainty approach has been recently treated in Yosef and Bel.[25]

Example 2.2. We consider the random coupled parabolic problems (1)–(4) with the initial boundary conditions

$$u(z,0) = f(z) = \begin{bmatrix} 0 \\ 0 \end{bmatrix}, \ \frac{\partial u}{\partial z}(0,t) = \begin{bmatrix} -g(t) \\ 0 \end{bmatrix} = \begin{bmatrix} -1 \\ 0 \end{bmatrix}, \tag{53}$$

and the random matrix coefficients

$$A(\xi) = \begin{bmatrix} 0 & a(\xi) \\ -a(\xi) & 0 \end{bmatrix}, \ B(\xi) = \nu(\xi) I = \begin{bmatrix} \nu(\xi) & 0 \\ 0 & \nu(\xi) \end{bmatrix}, \tag{54}$$

where the r.v. $a(\xi) > 0$ follows a Gaussian distribution of mean $\mu = 2$ and standard deviation $\sigma = 0.1$ truncated on the interval $[0.8, 1.2]$, that is, $a(\xi) \sim N_{[0.8,1.2]}(2, 0.1)$, and the r.v. $\nu(\xi) > 0$ has a gamma distribution of parameters $(4; 2)$ truncated on the interval $[0.5, 1.5]$, that is, $\nu(\xi) \sim Ga_{[0.5,1.5]}(4; 2)$. Both r.v.'s are considered independent ones. Observe that the random matrices $A(\xi) \in L_4^{2\times 2}(\Omega)$ and $B(\xi) \in L_8^{2\times 2}(\Omega)$ and verifying the moment condition (39) because the r.v.'s $a(\xi)$ and $b(\xi)$ are bounded. The function $g(t) = 1$ involves in the boundary condition (53) is in $L_8^{2\times 1}(\Omega)$ for each t and is continuous too. Furthermore, the random spectral condition (43) is satisfied because the r.v. $\nu(\xi) > 0$. The exact solution of problems (1)–(4) in its deterministic version is given by (29) with $g(s) = 1$. Figure 4 shows the numerical values of the expectation and the standard deviation of the exact solution s.p. (1)–(4) and (53)–(54) considering both at fixed time $t = 1$. Computations have been carried out by Mathematica©software version 11.3.0.0,[26] for Windows

TABLE 5 Timings for computing the numerical values of the expectation and the standard deviation of the exact solution s.p. (1)–(4) and (53)–(54) at time $t = 1$ in the spatial domain $0 \le z \le 5$ for $\Delta z = 0.1$

Statistical Moments	CPU, s
$\mathbb{E}[u_1(z,1)]$	18.2656
$\mathbb{E}[u_2(z,1)]$	20.4531
$\sqrt{\mathrm{Var}[u_1(z,1)]}$	7592.3800
$\sqrt{\mathrm{Var}[u_2(z,1)]}$	539.1560

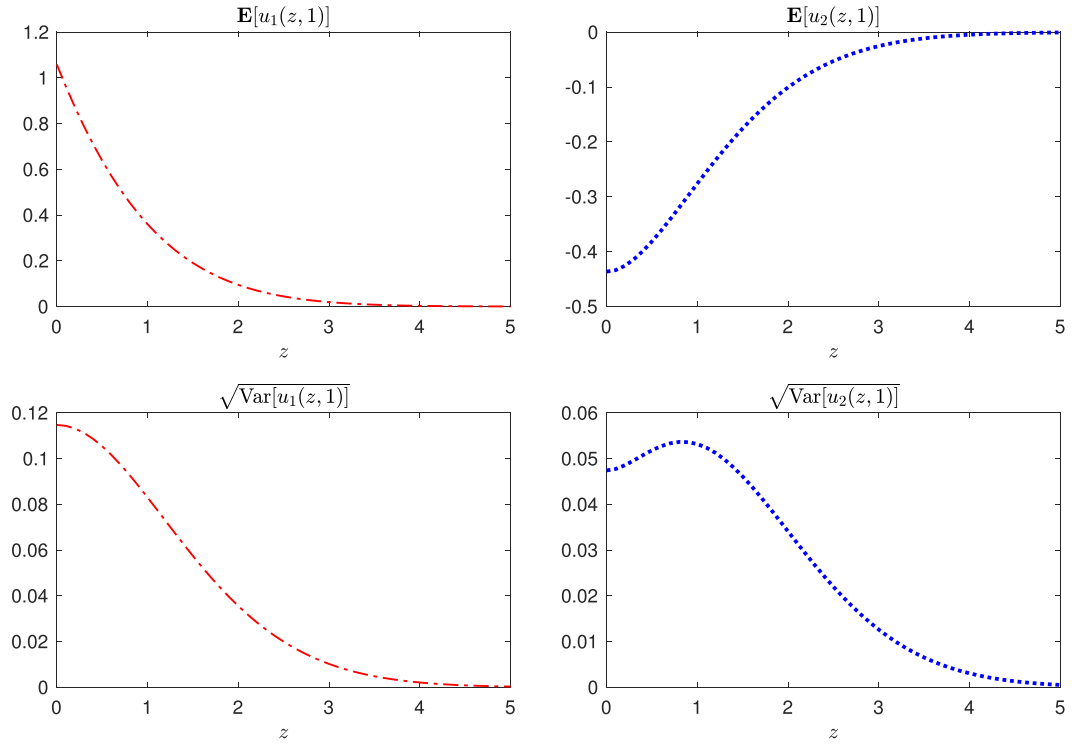

FIGURE 4 Expectation and the standard deviation at the time instant $t = 1$ of the exact solution s.p., $[u_1(z,t), u_2(z,t)]$, for the random coupled parabolic problems (1)–(4) and (53)–(54), considering the r.v.'s $a(\xi) \sim N_{[0.8,1.2]}(2, 0.1)$ and $\nu(\xi) \sim Ga_{[0.5,1.5]}(4; 2)$, and the spatial domain $z \in [0, 5]$ with step size $\Delta z = 0.1$ [Colour figure can be viewed at wileyonlinelibrary.com]

ξ_i	RMSE$\left(\mathbb{E}\left[\mathbf{Mid}_N(\boldsymbol{u}_{1,R}(z,1)(\xi_i))\right]\right)$	RMSE$\left(\mathbb{E}\left[\mathbf{Mid}_N(\boldsymbol{u}_{2,R}(z,1)(\xi_i))\right]\right)$	CPU, s
200	$4.9594e-03$	$2.8818e-04$	0.1205
400	$5.6568e-03$	$1.2430e-03$	0.2500
800	$4.8149e-03$	$1.2268e-03$	0.4531
1600	$4.9603e-03$	$4.5712e-04$	0.4844
3200	$5.0119e-03$	$4.4230e-04$	1.1406
6400	$4.7532e-03$	$8.8098e-04$	1.2188
12800	$4.8759e-03$	$1.2562e-04$	5.2656

TABLE 6 Root mean square errors (RMSEs) of the numerical approximations of the expectation (49) for the the solution s.p. (46) at $t = 1$ in $0 \leq z \leq 5$ with $\Delta z = 0.1$ varying the number of realizations ξ_i for $R = 20$ and $h = 0.05$ ($N = 400$)

ξ_i	RMSE$\left(\sqrt{\text{Var}\left[\mathbf{Mid}_N(\boldsymbol{u}_{1,R}(z,1)(\xi_i))\right]}\right)$	RMSE$\left(\sqrt{\text{Var}\left[\mathbf{Mid}_N(\boldsymbol{u}_{2,R}(z,1)(\xi_i))\right]}\right)$	CPU, s
200	$1.8818e-03$	$1.3906e-03$	0.6094
400	$2.7378e-04$	$1.9727e-04$	0.9531
800	$3.8938e-03$	$2.3218e-03$	1.9844
1600	$5.0547e-04$	$3.2676e-04$	6.9531
3200	$3.1779e-04$	$1.1304e-04$	19.0313
6400	$6.6312e-04$	$3.6929e-04$	55.1094
12800	$2.9489e-04$	$1.5663e-04$	186.484

TABLE 7 Root mean square errors (RMSE) of the numerical approximations of the standard deviation (50) for the solution s.p. (46) at $t = 1$ in $0 \leq z \leq 5$ with $\Delta z = 0.1$ varying the number of realizations ξ_i for $R = 20$ and $h = 0.05$ ($N = 400$)

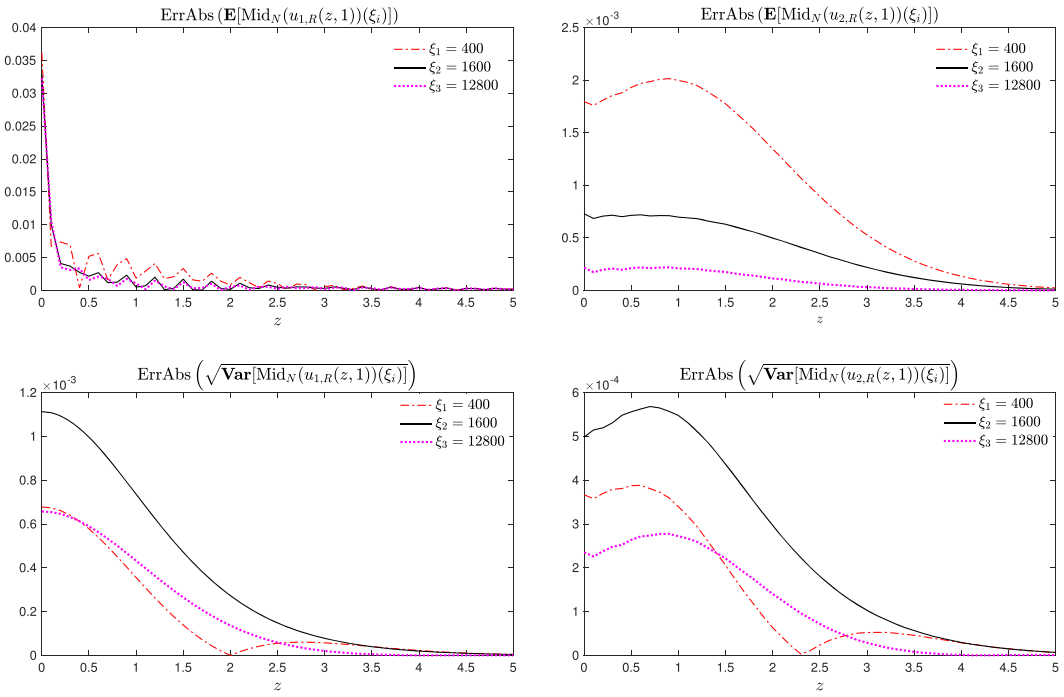

FIGURE 5 Absolute errors of the expectation and the standard deviation for both components of the approximate solution s.p. (48) at $t = 1$ fixing $R = 20$ and $h = 0.05$ ($N = 400$) in (49)–(50) but varying the number of simulations $\xi_i = \{400, 1600, 12800\}$. The spatial domain is $z \in [0, 5]$ with $\Delta z = 0.1$ [Colour figure can be viewed at wileyonlinelibrary.com]

10Pro (64-bit) Intel(R) Core(TM) i7-7820X CPU, 3.60 GHz 8 kernels. In Table 5, we show the timings (CPU time spent in the Wolfram Language kernel) to compute both statistical moments of the exact solution plotted in Figure 4.

Numerical convergence of the statistical moments (49)–(50) of the approximate solution s.p. (48) based on the mid-point Riemann sum quadrature and Monte Carlo technique is illustrated in the following way. Tables 6 and 7 collect the RMSEs for the numerical expectation and the standard deviation, respectively, for several number of realizations ξ_i in the Monte Carlo method. In this first experiment, suitable values of truncation endpoint R and step size h suggested by the deterministic Example 2.1 have been fixed. Figure 5 illustrates the decreasing trend of the absolute errors of the approximations to the expectation, $\mathbb{E}[\text{Mid}_N\,(u_R(z,t)(\xi))]$ (49), and the standard deviation, $\sqrt{\text{Var}[\text{Mid}_N\,(u_R(z,t)(\xi))]}$

TABLE 8 Root mean square errors (RMSE) of the numerical approximations of the expectation (49) for the solution s.p. (46) at $t = 1$ in $0 \leq z \leq 5$ with $\Delta z = 0.1$. The number of realizations $\xi = 1600$ and $h = 0.05$ is fixed and the size of the integration domain R_i varies

R_i	RMSE$\left(\mathbb{E}\left[\text{Mid}_N(u_{1,R_i}(z,1)(\xi))\right]\right)$	RMSE$\left(\mathbb{E}\left[\text{Mid}_N(u_{2,R_i}(z,1)(\xi))\right]\right)$	CPU, s
5	$2.2870e-02$	$7.0643e-04$	0.1719
10	$1.0113e-02$	$4.6269e-04$	0.3281
15	$6.6053e-03$	$4.5785e-04$	0.5938
20	$4.9603e-03$	$4.5712e-04$	0.6406
25	$3.9572e-03$	$4.5689e-04$	1.3750

TABLE 9 Root mean square errors (RMSEs) of the numerical approximations of the expectation standard deviation (50) for the solution s.p.(46) at $t = 1$ in $0 \leq z \leq 5$ with $\Delta z = 0.1$. The number of realizations $\xi = 1600$ and $h = 0.05$ is fixed and the size of the integration domain R_i varies

R_i	RMSE$\left(\sqrt{\text{Var}\left[\text{Mid}_N(u_{1,R_i}(z,1)(\xi))\right]}\right)$	RMSE$\left(\sqrt{\text{Var}\left[\text{Mid}_N(u_{2,R_i}(z,1)(\xi))\right]}\right)$	CPU, s
5	$5.0618e-04$	$3.4636e-04$	3.3594
10	$5.0549e-04$	$3.2624e-04$	13.1406
15	$5.0547e-04$	$3.2662e-04$	34.6875
20	$5.0547e-04$	$3.2676e-04$	80.4688
25	$5.0547e-04$	$3.2681e-04$	123.1250

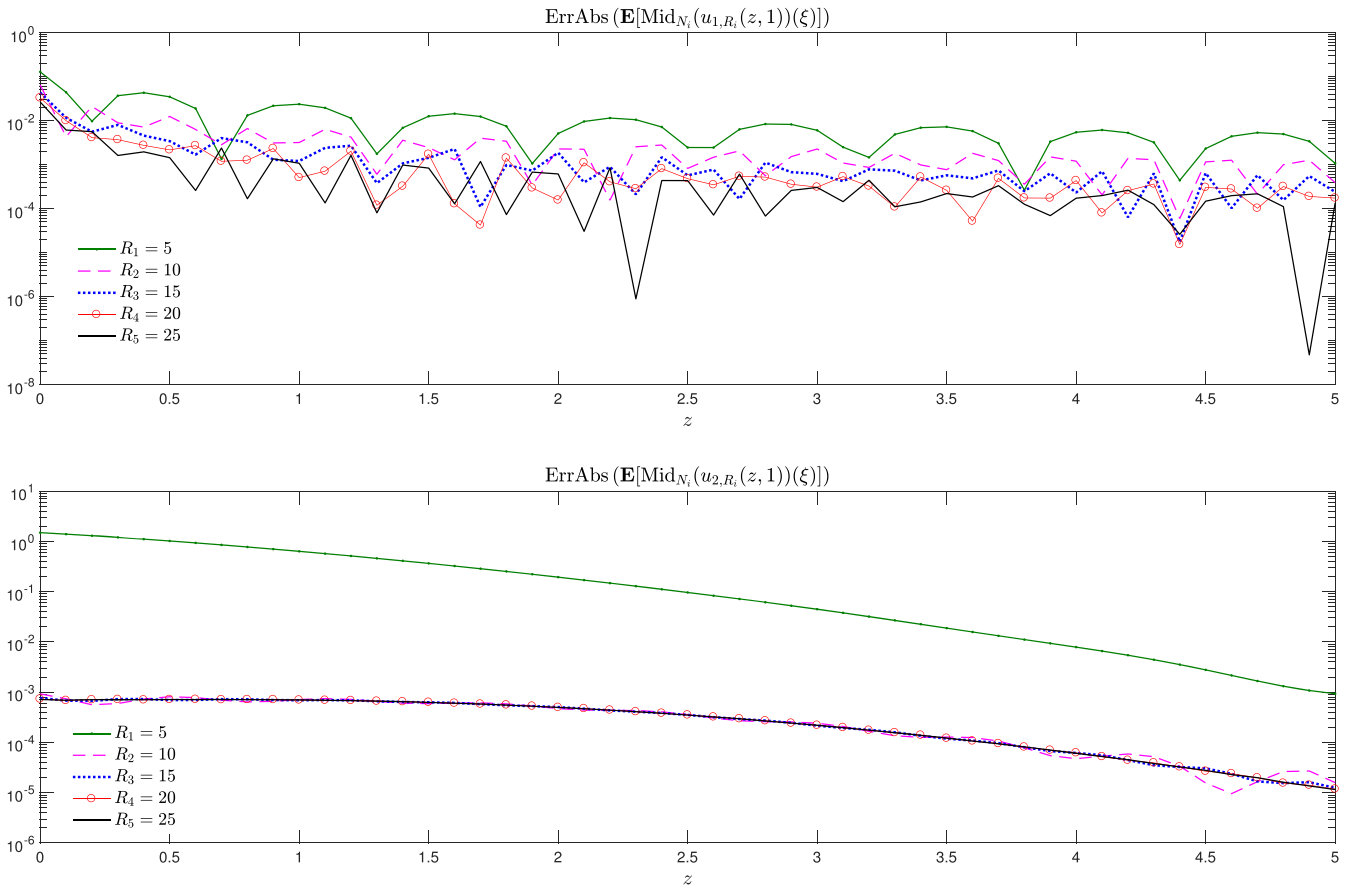

FIGURE 6 Absolute errors of the expectation and the standard deviation for both components of the approximate solution s.p. (48) at $t = 1$ with logarithmic scale for the y axis. The number of simulations $\xi = 1600$ and the step size $h = 0.05$ in (49)–(50) are fixed, but the size of the integration domain, R, varies $R_i = \{5, 10, 15, 20, 25\}$. The spatial domain is $z \in [0, 5]$ with $\Delta z = 0.1$ and $N_i = \{100, 200, 300, 400, 500\}$ so that $R = Nh$ [Colour figure can be viewed at wileyonlinelibrary.com]

TABLE 10 Comparison of the root mean square errors (RMSEs) of the expectations for the random midpoint quadrature, (49) and random trapezoidal quadrature (51) at $t = 1$ in $0 \leq z \leq 5$ with $\Delta z = 0.1$. The number of realizations $\xi = 1600$ and $R = 20$ is fixed and the step size h_i of the integration varies

h_i	$\mathbf{RMSE}\left(\mathbb{E}\left[\mathbf{Mid}_N[\boldsymbol{u}_{1,R}(z,1)(\xi),\ \boldsymbol{u}_{2,R}(z,1)(\xi)]\right]\right)$	$\mathbf{RMSE}\left(\mathbb{E}\left[\mathbf{Trap}_N[\boldsymbol{u}_{1,R}(z,1)(\xi),\ \boldsymbol{u}_{2,R}(z,1)(\xi)]\right]\right)$
1	$[7.23250e-02, 6.82348e-02]$	$[7.22725e-02, 6.81724e-02]$
0.05	$[4.96031e-03, 4.57117e-04]$	$[4.96647e-03, 4.57117e-04]$
0.025	$[4.96029e-03, 4.57117e-04]$	$[4.96337e-03, 4.57118e-04]$

TABLE 11 Comparison of the root mean square errors (RMSEs) of the standard deviations for the random midpoint quadrature (50) and random trapezoidal quadrature (52), at $t = 1$ in $0 \leq z \leq 5$ with $\Delta z = 0.1$. The number of realizations $\xi = 1600$ and $R = 20$ is fixed and the step size h_i of the integration varies

h_i	$\mathbf{RMSE}\left(\sqrt{\mathbf{Var}_N\left[\mathbf{Mid}_N[\boldsymbol{u}_{1,R}(z,1)(\xi),\ \boldsymbol{u}_{2,R}(z,1)(\xi)]\right]}\right)$	$\mathbf{RMSE}\left(\sqrt{\mathbf{Var}\left[[\mathbf{Trap}_N[\boldsymbol{u}_{1,R}(z,1)(\xi),\ \boldsymbol{u}_{2,R}(z,1)(\xi)]\right]}\right)$
1	$[2.16066e-02, 1.78262e-02]$	$[2.27856e-02, 1.97827e-02]$
0.05	$[5.05470e-04, 3.26758e-04]$	$[5.05470e-04, 3.26757e-04]$
0.025	$[5.05470e-04, 3.26758e-04]$	$[5.05470e-04, 3.26757e-04]$

(50), when the simulations ξ_i by Monte Carlo increase. If more precision is required, it should be increasing the values of parameters R and h (or N) rather than increasing the number of simulations ξ_i.

Second, by varying the length of R for both h and the number of realizations ξ fixed, the computed RMSEs are shown in Tables 8 and 9. We have chosen $\xi = 1600$ realizations because the results obtained in the previous study are sufficiently accurate. Figure 6 shows how the approximate expectation, $\mathbb{E}[\mathrm{Mid}_N\left(u_{R_i}(z,t)(\xi)\right)]$ (49), improves when the size of the integration domain R_i increases.

The CPU times of the numerical experiments exhibit the efficiency of the proposed method versus the long times spent to compute the statistical moments in Table 5.

The comparative Tables 10 and 11 collect the RMSEs for the expectation and the standard deviation using both methods midpoint and trapezoidal. The results shown are very similar in both cases.

4 | CONCLUSIONS

This paper shows that the integral transform method combined with numerical integration and Monte Carlo technique is useful to deal with random systems of PDEs. Although here, we consider parabolic type systems and cosine Fourier transform, the ideas are applicable to other systems and other integral transforms. The numerical integration must consider the possible oscillatory nature of the involved integrals. This approach is a manageable alternative to deal with the computational complexity derived from the treatment of random models versus the iterative methods.

The main advantage of the present method is twofold. First, taking advantage of the integral transform method, we obtain an integral form of the solution of the random original problem. Second, to implement efficient random quadrature rules for the approximation of the involved oscillatory type integral. Accuracy and computational cost are illustrated with examples.

ORCID

María Consuelo Casabán https://orcid.org/0000-0002-5708-5709
Rafael Company https://orcid.org/0000-0001-5217-1889

Vera N. Egorova https://orcid.org/0000-0002-3024-3033
Lucas Jódar https://orcid.org/0000-0002-9672-6249

REFERENCES

1. Bäck J, Nobile F, Tamellini L, Tempone R. Stochastic spectral galerkin and collocation methods for PDEs with random coefficients: a numerical comparison. In: Hesthaven J, Rønquist E, eds. *Spectral and High Order Methods for Partial Differential Equations, Lecture Notes in Computational Science and Engineering*. Vol 76. Berlin, Heidelberg: Springer; 2011.
2. Bachmayr M, Cohen A, Migliorati G. Sparse polynomial approximation of parametric elliptic PDEs. *Part I: affine coeff ESAIM M2AN*. 2017;51(1):321–339.
3. Ernst O, Sprungk B, Tamellini L. Convergence of sparse collocation for functions of countably many Gaussian random variables (with application to elliptic PDEs). *SIAM J Num Anal*. 2018;56(2):877–905.
4. Sheng D, Axelsson K. Uncoupling of coupled flows in soil-a finite element method. *Int J Num Anal Met Geomech*. 1995;19(8):537–553.
5. Mitchell JK. Conduction phenomena: from theory to geotechnical practice. *Géotechnique*. 1991;41(3):299–340.
6. Metaxas AC, Meredith RJ. *Institution of Electrical Engineers. Industrial microwave heating, Peter Peregrinus Ltd. on behalf of the Institution of Electrical Engineers*. London; 1983.
7. Das PK. *Optical Signal Processing*. Berlin Heidelberg: Springer-Verlag; 1991.
8. Ekman VW. On the influence of the Earth's rotation on ocean-currents. Arkiv for Matematik. *Astronomi och Fysik*. 1905;2(11):1–52.
9. Yosef AHG, Bel G. Energy transfer of surface wind-induced currents to the deep ocean via resonance with the Coriolis force. *J Marine Syst*. 2017;167:93–104.
10. Stacey Weston M. *Fusion Plasma Analysis*: John Wiley & Sons Inc; 1981.
11. Hodgkin AL, Huxley AF. A quantitative description of membrane current and its application to conduction and excitation in nerve. *J Phys*. 1952;117(4):500–544.
12. Winfree AT. *When Time Breaks Down: The Three-Dimensional Dynamics of Electrochemical Waves and Cardiac Arrhythmias*. Princeton, NJ, USA: Princeton University Press; 1987.
13. Galiano G. On a cross-diffusion population model deduced from mutation and splitting of a single species. *Comput Math Appl*. 2012;64(6):1927–1936.
14. Casabán MC, Company R, Jódar L. Numerical solutions of random mean square Fisher–KPP models with advection. *Math Methods Appl Sci*. 2019.
15. Casabán MC, Company R, Jódar L. Numerical integral transform methods for random hyperbolic models with a finite degree of randomness. *Math*. 2019;7(9):853.
16. Shampine LF. Vectorized adaptive quadrature in MATLAB. *J Comput Appl Math*. 2008;211(2):131–140.
17. Iserles A. On the numerical quadrature of highly-oscillating integrals I: Fourier transforms. *IMA J Num Anal*. 2004;24(3):365–391.
18. Ma J, Liu H. On the convolution quadrature rule for integral transforms with oscillatory Bessel kernels. *Symmetry*. 2018;10(7).
19. Jódar L, Goberna D. Exact and analytic numerical solution of coupled diffusion problems in a semi-infinite medium. *Comput Math Appl*. 1996;31(9):17–24.
20. Jódar L, Goberna D. A matrix D'Alembert formula for coupled wave initial value problems. *Comp Math Appl*. 1998;35(9):1–15.
21. Davis PJ, Rabinowitz P. *Computer Science and Applied Mathematics*. San Diego: Academic Press, Inc.; 1984.
22. Dahlquist G. *Stability and Error Bounds in the Numerical Integration of Ordinary Differential Equations*. Stockholm: Almqvist & Wiksells; 1958.
23. Ostrowski AM. A quantitative formulation of Sylvester's law of inertia. *Proc Nat Acad Sci Unit Stat Amer*. 1959;45(5):740–44.
24. The MathWorks Inc.. *Matlab (R2019b)*. Natick, Massachusetts: The Mathworks, Inc.; 2019.
25. Yosef AHG, Bel G. The effect of stochastic wind on the infinite depth Ekman layer model. *EPL*. 2015;111(3):39001.
26. Wolfram Research Inc. *Mathematica*, Version 11.3. Champaign, United States; 2018.